Sugar Conformations in DNA and RNA−DNA Triple Helices Determined by FTIR Spectroscopy: Role of Backbone Composition

C. Dagneaux, J. Liquier, and E. Taillandier*

Laboratoire CSSB, URA CNRS 1430, UFR Santé, Médecine et Biologie Humaine, Université Paris Nord, 74 rue Marcel Cachin, F-93012 Bobigny Cedex, France

Received July 5, 1995; Revised Manuscript Received September 18, 1995[⊗]

ABSTRACT: We have studied the effect of the nature of the third-strand sugar (ribose or deoxyribose) on the geometry and stability of triple helices with a pyrimidine motif targeting the polypurine tract of the Friend murine retrovirus. Comparison between triplexes containing a third strand formed by a deoxy 13mer d(TCT_5C_6), the same oligomer but with C_5-methylated cytosines d($T^{5me}CT_5{}^{5me}C_6$), and an analogous modified 13mer RNA $^{2'Ome}$r(UCU_5C_6) shows that the sugar conformations of the different triple helices, determined by FTIR spectroscopy, differ depending on nature of the third-strand sugar. Pyrimidine*purine−pyrimidine triple-helix formation with the third-strand RNA and the duplex as DNA appears to be associated with a conversion of the duplex part from a B-form secondary structure with S-type sugars to a geometry in which the polypurine strand sugars adopt an N-type conformation. Thermal dissociation of the triplexes was studied by UV absorbance spectroscopy. The most stable triple helix is obtained when the third strand contains 2′-*O*-methylated ribose sugars.

Research in the area of triple-helix formation has recently called the attention to possible different conformational families of triplexes depending on backbone composition (Han & Dervan, 1994; Semerad & Maher, 1994). Some of the questions that should be answered in view of their numerous therapeutical potentialities are: what is the importance of the targeted double-stranded geometry? How can a third strand fit into the duplex major groove, and, consequently, will there be any structural modifications in the duplex? And is there a role played by third-strand composition (DNA or RNA) in particular on triple-helix stability? Dramatic effects of DNA/RNA strand substitution on triple-helix stability have been reported, although the results apparently differ, possibly due to differences in the types of systems studied (hairpin duplexes with a separate third strand of identical length, long-stranded duplexes with short third strands, circularized duplexes, etc.; (Roberts & Crothers, 1992; Escudé et al., 1993; Han & Dervan, 1993; Wang & Kool, 1994, 1995; Mc Donald & Maher, 1995). However, very little structural data concerning triple helices that contain both DNA and RNA strands are available.

In the triple-helical pattern termed the pyrimidine motif, the third strand binds in the large groove of the targeted duplex through Hoogsteen-type hydrogen bonds (T*A−T and C^+*G−C triplets) (Rajagopal & Feigon, 1989; de los Santos et al., 1989; Radhakrishnan & Patel, 1994a,b). In the present work the chosen target is the polypurine tract AGA_5G_6 of the Friend retrovirus (Friend, 1957), which is highly conserved in other viral systems. A particular feature of this sequence is that it contains a long stretch of adjacent guanines. The structure of triple helices formed by addition of either a third deoxyribo or a third ribo strand to the d(AGA_5G_6)−d(C_6T_5CT) duplex has been studied by Fourier transform infrared spectroscopy and thermal dissociation followed by UV spectroscopy. We have used three different oligonucleotides as the third strand: a 13mer DNA d(TCT_5C_6), the same oligomer but with C_5-methylated cytosines d($T^{5me}CT_5{}^{5me}C_6$), and a modified 13mer RNA $^{2'Ome}$r(UCU_5C_6) [base or sugar chemical modifications, such as cytosine C_5 methylation (Povsic et al., 1989; Sun & Hélène, 1993) or 2′-*O*-ribose methylation (Shimizu et al., 1991; Escudé et al., 1992) are supposed to induce triple-helix stabilization].

FTIR spectroscopy has proved to be well suited for the study of nucleic acid conformations (Taillandier & Liquier, 1992) and in the case of triple helices allows one to follow the formation of the triplexes, evidence interactions at the level of functional groups such as base carbonyls and purine N_7 sites and characterize sugar geometries in these structures (Liquier et al., 1993). This technique has unambiguously shown the existence of S-type sugars (C2′endo, B-family form) in pyrimidine*purine−pyrimidine triple helices and in particular was the first to evidence that in the (dT*dA−dT)$_n$ triplex all sugars were in S-type geometry (Liquier et al., 1991). We show here that either of the three 13mers can form a triple helix with the d(AGA_5G_6)−d(C_6T_5CT) duplex; however, sugar conformations in these triplexes are different. We observe mainly S-type sugars in triple helices formed with a third deoxy strand, while N-type sugars (C3′endo, A-family form) are mainly found in triple helices containing a ribo third strand. In this latter case the purine strand sugars undergo a S-type → N-type conformational reorientation. UV thermal denaturation experiments show that the most stable triplex is obtained with the $^{2'Ome}$r(UCU_5C_6) third strand, followed by d($T^{5me}CT_5{}^{5me}C_6$) and finally d(TCT_5C_6).

MATERIALS AND METHODS

Sample Preparation. Oligonucleotides were purchased from Genosys. Purity was controlled by HPLC, and salt content was controlled by elution on a G10 column.

* Author to whom correspondence should be addressed.

[⊗] Abstract published in *Advance ACS Abstracts,* November 15, 1995.

[1] In the triple-helix notation, "*" represents third-strand binding while "−" represents the Watson−Crick base pairing of the target duplex.

0006-2960/95/0434-16618$09.00/0

Concentrations of stock solutions were determined spectrophotometrically (UV absorbance around 260 nm) using computed sequence dependent extinction coefficients given by a nearest-neighbor model (Fasman, 1975) [7610 L mol^{-1} cm^{-1} for d(C_6T_5CT); 7680 L mol^{-1} cm^{-1} for d(TCT_5C_6) and d($T^{5me}CT_5{}^{5me}C_6$); 8250 L mol^{-1} cm^{-1} for $^{2'Ome}$r(UCU_5C_6); 11 300 L mol^{-1} cm^{-1} for d(AGA_5G_6)]. The oligomer solutions were heated at 85 °C for 5 min. The duplex was prepared by equimolecular mixing of single-strand stock solutions and left to equilibrate for 24 h at room temperature. The third strand was then added at neutral pH. Further pH adjustment was obtained by addition of dilute HCl solution. For FTIR spectroscopy, samples were deposited between ZnSe windows without spacer. To record spectra in D_2O solutions, samples originally prepared in H_2O were slowly evaporated under nitrogen and redissolved in the same volume of deuterated solvent. Measurement of pH was performed directly in the sample studied by FTIR spectroscopy using a microprobe MI 4152 from Microelectrodes Inc. (usual volume of sample between 1 and 2 μL). PH values given in the text correspond to measurements performed in H_2O solutions prior to hydrogen−deuterium exchange. For UV spectroscopy samples were prepared in 100 mM NaCl at a concentration of 5 μM strand.

Infrared Spectroscopy. FTIR spectra were recorded with a Perkin-Elmer 1760 spectrophotometer coupled to a Perkin-Elmer 7700 minicomputer. 25 scans were usually accumulated. Data were treated on an IBM PS2 computer using the Galaxy Spectra Calc program (solvent substraction, multiple-point base line correction and spectral normalization using the phosphate symmetric stretching vibration band located around 1090 cm^{-1} as the internal standard).

UV Spectroscopy. Absorption spectra and absorbance versus temperature profiles (measured at the maximum of the absorption band around 262 nm and at 330 nm) were recorded with a Kontron Uvikon 941 spectrophotometer. The absorbance at 330 nm (zero reference absorption) was substracted from that at 262 nm. Absorption data were averaged for 60 s. Temperature of the cell holder (sample and reference) was varied (0.1 °C per minute) by circulating liquid using a Huber water bath controlled by a Huber PD415 temperature programmer.

RESULTS

Triple-Helix Formation. Triple-helix formation can be followed by FTIR spectroscopy using absorption bands assigned to base in-plane double-bond vibrations located in the 1800−1500 cm^{-1} spectral domain, sensitive to base−base interactions. Infrared markers reflecting formation of T*A−T and C$^+$*G−C base triplets were found for triple helices formed by interstrand monobase oligo and polynucleotides (Liquier et al., 1991; Howard et al., 1992; Akhebat et al., 1992) and successfully used to characterize inter- and intrastrand triple-helix formation in oligomers containing simultaneously different types of pyrimidine* purine−pyrimidine base triplets (Dagneaux et al., 1994; Klinck et al., 1994). Formation of pyrimidine*purine−pyrimidine base triplets involving an adenine, such as U*A−U, U*A−T, T*A·U, or T*A−T, is characterized by a drastic decrease of the adenine band located around 1622 cm^{-1}, assigned to C=C and C=N ring stretching and ND_2 bending vibrations. Existence of C$^+$*G−C base triplets is evidenced

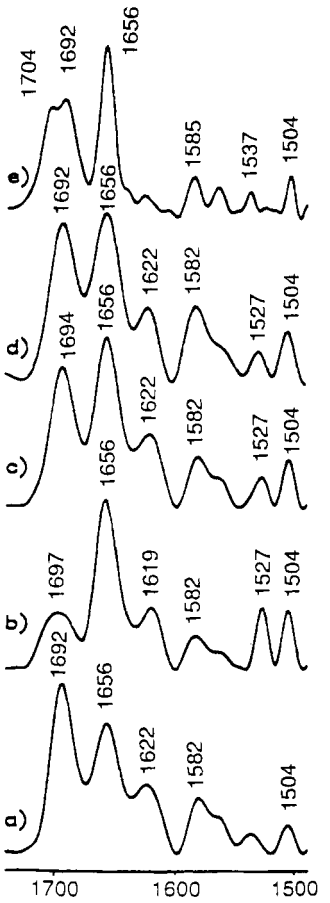

FIGURE 1: Formation of the $^{2'Ome}$r($UC^+U_5C^+_6$)*d(AGA_5G_6)−d(C_6T_5CT) triple helix. FTIR spectra recorded in D_2O solutions of (a) d(AGA_5G_6)−d(C_6T_5CT), double-stranded helix, pH 7; (b) $^{2'Ome}$r(UCU_5C_6), single strand, pH 7; (c) computed curve addition after normalization of spectra a and b; (d) equimolecular mixture of d(AGA_5G_6)−d(C_6T_5CT) and $^{2'Ome}$r(UCU_5C_6), pH 7; (e) equimolecular mixture of d(AGA_5G_6)−d(C_6T_5CT) and $^{2'Ome}$r(UCU_5C_6), pH 4, triple helix. The spectral region presented contains the in-plane double-bond stretching vibrations of the bases. Absorbance scale in arbitrary units.

by the emergence of a high-wavenumber absorption band (above 1700 cm^{-1}) assigned to a non-hydrogen-bonded C_2=O_2 carbonyl stretching vibration of third-strand protonated cytosines involved in Hoogsteen-type base pairing with guanines of the Watson−Crick duplex.

Figure 1 presents evidence of the formation of the $^{2'Ome}$r($UC^+U_5C^+_6$)*d(AGA_5G_6)−d(C_6T_5CT) triple helix. FTIR spectra recorded in D_2O solution of the d(AGA_5G_6)−d(C_6T_5CT) duplex, of the $^{2'Ome}$r(UCU_5C_6) third strand, and of the stoichiometric mixture (one third-strand molecule per duplex) recorded at neutral and acidic pH are respectively presented in Figure 1a,b,d,e. Curve c was obtained by addition after normalization of spectra a and b (duplex and third strand). As can be seen, this "simulated" spectrum is identical to the spectrum of the mixture recorded at neutral pH, showing that in these conditions no interaction takes place between duplex and single strand. When the pH is decreased, several modifications in the FTIR spectrum are observed (comparison of spectra shown Figure 1d,e). We no longer observe the adenine absorption band that was detected at 1622 cm^{-1} at neutral pH. This reflects formation of U*A−T base triplets. The emergence of a new contribution at 1704 cm^{-1} is indicative of formation of C$^+$*G−C base triplets. This is confirmed by the disappearance of the

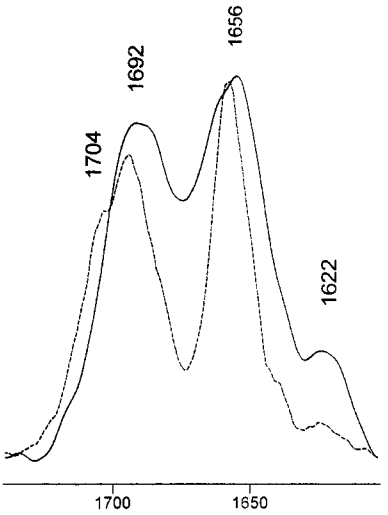

FIGURE 2: FTIR spectra recorded in D_2O solutions of the equimolecular mixture of $d(AGA_5G_6)-d(C_6T_5CT)$ and $^{2'Ome}r(UCU_5C_6)$, pH 5.4; solid line, spectrum obtained after decreasing the pH of the mixture from pH 7 (triple helix not formed); dashed line, spectrum obtained after increasing the pH of the mixture from pH 4 (triple helix formed).

1527 cm^{-1} cytosine band, which shows that third-strand cytosines are involved in hydrogen bonding, and by the presence of a band at 1537 cm^{-1} assigned to a vibration involving motions of purine N7 sites, which are now hydrogen bonded. The $^{2'Ome}r(UC^+U_5C^+_6)*d(AGA_5G_6)-d(C_6T_5CT)$ triple helix was formed in low pH conditions necessary to protonate third-strand cytosines. In intermediate conditions, at pH 5.4, two different FTIR spectra were obtained, depending how this pH value was reached. The first one (Figure 2, solid line), recorded after decreasing the pH from pH 7, presented an adenine contribution at 1622 cm^{-1} and no characteristic cytosine absorption band at 1704 cm^{-1}, showing that the triple helix was not formed. The second one (Figure 2, dashed line), recorded after increasing the pH from pH 4 was the same as that obtained at pH 4, showing that once the triple helix is formed, it is stable at higher pH values up to pH 5.4. If the pH is still increased, we observe at pH 6.2 that the triplex is no longer formed (spectrum not shown).

In the case of stoichiometric mixtures of the $d(AGA_5G_6)-d(C_6T_5CT)$ duplex either with $d(TCT_5C_6)$ or with $d(T^{5me}CT_5{}^{5me}C_6)$, a decrease of pH induces formation of $d(TC^+T_5C^+_6)*d(AGA_5G_6)-d(C_6T_5CT)$ or $d(T^{5me}C^+T_5{}^{5me}C^+_6)*d(AGA_5G_6)-d(C_6T_5CT)$ triple helices evidenced, as described in detail above for the $^{2'Ome}r(UC^+U_5C^+_6)*d(AGA_5G_6)-d(C_6T_5CT)$ triple helix, by a decrease of the 1622 cm^{-1} adenine band, the emergence of a protonated cytosine contribution around 1715 cm^{-1} and of a guanosine contribution at 1537 cm^{-1} (spectra not shown).

Formation of pyrimidine*purine−pyrimidine triple helices studied here requires the establishment of an hydrogen bond between the third-strand pyrimidine base and the purine (either adenine or guanine) N_7 site. FTIR spectroscopy gives us the opportunity to detect such interactions by following the displacement of absorption bands involving motions of the N_7 atom. A very sensitive absorption band is observed around 1490 cm^{-1} and is assigned to a N_7C_8H bending vibration. Any modification in the position of this band will reflect an interaction on the N_7 site. Figure 3 presents the FTIR spectra (in H_2O solutions) of the stoichiometric mixture

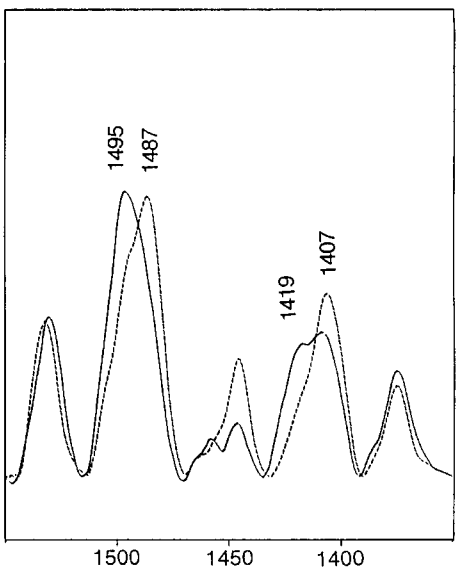

FIGURE 3: FTIR spectra recorded in H_2O solutions of the stoichiometric mixture of $d(AGA_5G_6)-d(C_6T_5CT)$ and $^{2'Ome}r(UCU_5C_6)$ at pH 7 (solid line) and pH 5 (dashed line).

of the duplex with $^{2'Ome}r(UCU_5C_6)$ at neutral pH (solid line) and at pH 5 (dashed line). At neutral pH the N_7C_8H bending vibration is observed at 1495 cm^{-1}. When the pH is descreased, this band is shifted to lower wavenumbers (1487 cm^{-1}), showing the existence of an interaction on the purine N_7 site, correlated with triple-helix formation.

The relative stabilities of the triplexes have been examined by UV thermal denaturation. Figure 4 presents normalized denaturation profiles of the different triple helices in 100 mM NaCl at pH 5 obtained by increasing the temperature from 10 °C, as well as the corresponding derivative curves. Melting profiles of the triplexes show notable differences, depending on the third strand used. We observe that C_5 methylation of third-strand cytosines induces a stabilization of the triplex [25 °C for $d(T^{5me}CT_5{}^{5me}C_6)$ instead of 18 °C for $d(TCT_5C_6)$] while duplex melting in both cases occurs at 37 °C. A monophasic transition reflecting simultaneous third strand and duplex dissociation is observed at higher temperature (46 °C) when the third strand is modified RNA $^{2'Ome}r(UCU_5C_6)$.

Sugar Conformations. FTIR spectroscopy allows direct characterization of sugar geometries in nucleic acids. Absorption bands, markers of N-type (including the A-family form C3′endo/*anti* geometry) and S-type (including the B-family form C2′endo/*anti* geometry) sugars, have been obtained. They are quite general, independent of base composition or sequence. Spectra of structures containing N-type sugars present a strong absorption band around 865 cm^{-1}. The S-type sugar marker band is observed around 840 cm^{-1} (Taillandier & Liquier, 1992). These marker bands have been used to characterize sugar geometries in triple helices. When in a triple helix containing only deoxy strands the third deoxy strand is replaced by a ribose strand, for instance in $(rU*dA-dT)_n$ or in $(rC^+*dG-dC)_n$, the emergence of a band around 865 cm^{-1} or the disappearance of the 829 cm^{-1} band reflects a partial reorientation of sugars from an S-type to a N-type conformation (Liquier et al., 1991; Akhebat et al., 1992). In triplexes containing ribose sugars in all three strands no absorption band is observed around 840 cm^{-1}, showing that all sugars are in N-type conformation.

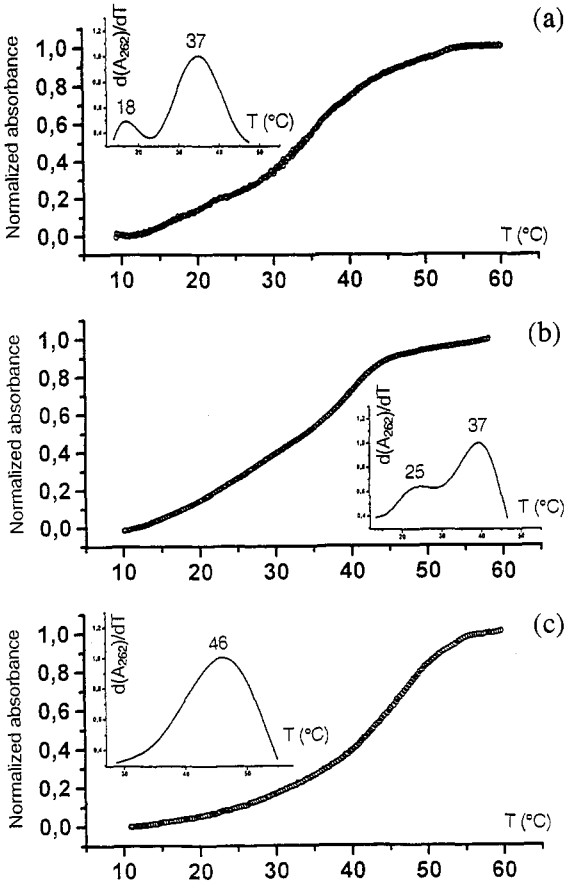

FIGURE 4: Normalized denaturation profiles in 100 mM NaCl, pH 5, and first-derivative curves $d(A_{262})/dT$ of (a) $d(TC^+T_5C^+_6)$*$d(AGA_5G_6)$−$d(C_6T_5CT)$ triplex, (b) $d(T^{5me}C^+T_5{}^{5me}C^+_6)$*$d(AGA_5G_6)$−$d(C_6T_5CT)$ triplex, and (c) $^{2'Ome}r(UC^+U_5C^+_6)$*$d(AGA_5G_6)$−$d(C_6T_5CT)$ triplex.

Figure 5 presents FTIR spectra recorded in H_2O solution of the single $d(C_6T_5CT)$ strand (Figure 5a), of the $d(AGA_5G_6)$−$d(C_6T_5CT)$ duplex (Figure 5b), and of the $d(TC^+T_5C^+_6)$*$d(AGA_5G_6)$−$d(C_6T_5CT)$ (Figure 5c), $d(T^{5me}C^+T_5{}^{5me}C^+_6)$*$d(AGA_5G_6)$−$d(C_6T_5CT)$ (Figure 5d), and $^{2'Ome}r(UC^+U_5C^+_6)$*$d(AGA_5G_6)$-$d(C_6T_5CT)$ (Figure 5e) triple helices. For comparison the spectrum of the equimolecular mixture of $^{2'Ome}r(UC^+U_5C^+_6)$ and $d(AGA_5G_6)$−$d(C_6T_5CT)$ at pH 7 is given Figure 5f. We can first notice that the sugar geometry in the original duplex is exclusively S-type, as expected for double-stranded DNA containing all four bases, in solution. This is clearly shown by the absorption band observed at 840 cm^{-1}. When a third deoxyribonucleic strand is added and the pH is decreased, both dT*dA−dT and dC^+*dG−dC entities are formed in similar amounts (six dT*dA−dT triplets versus seven dC^+*dG−dC triplets). Therefore we expect, concerning sugar geometries, to observe simultaneously S- and N-type sugars. The $(dT*dA-dT)_5$ stretch should present an FTIR spectrum similar to that of $(dT*dA-dT)_n$, with exclusively S-type sugars, while the $(dC^+*dG-dC)_6$ stretch should present an FTIR spectrum similar to that of $(dC^+*dG-dC)_n$ with about one-third of S-type sugars. In fact, FTIR spectra of both $d(TC^+T_5C^+_6)$*$d(AGA_5G_6)$−$d(C_6T_5CT)$ (Figure 5c) and $d(T^{5me}C^+T_5{}^{5me}C^+_6)$*$d(AGA_5G_6)$−$d(C_6T_5CT)$ (Figure 5d) triple helices contain a strong absorption band around 840 cm^{-1} and a weak contribution at 865 cm^{-1}, showing that sugars mainly adopt an S-type conformation.

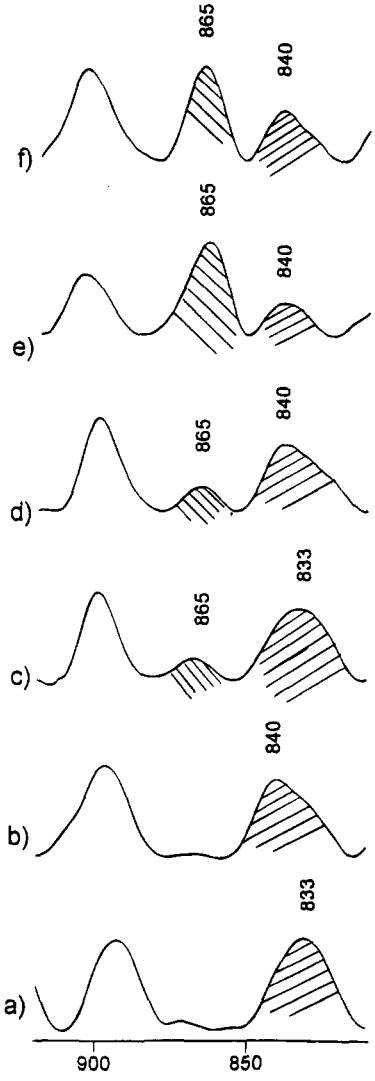

FIGURE 5: FTIR spectra recorded in H_2O solutions presented in the spectral domain containing the absorption bands characteristic of the sugar conformations of (a) $d(C_6T_5CT)$, single strand, pH 7; (b) $d(AGA_5G_6)$−$d(C_6T_5CT)$, duplex, pH 7; (c) $d(TC^+T_5C^+_6)$*$d(AGA_5G_6)$−$d(C_6T_5CT)$, triplex, pH 5; (d) $d(T^{5me}C^+T_5{}^{5me}C^+_6)$*$d(AGA_5G_6)$−$d(C_6T_5CT)$, triplex, pH 5; (e) $^{2'Ome}r(UC^+U_5C^+_6)$*$d(AGA_5G_6)$−$d(C_6T_5CT)$, triplex, pH 5; (f) stoichiometric mixture of $d(AGA_5G_6)$−$d(C_6T_5CT)$ and $^{2'Ome}r(UCU_5C_6)$ at pH 7. Characteristic absorption bands of sugar geometries are hatched: N-type, \\\\; S-type, ////.

In the case of the triple helix prepared with a ribose third strand, both absorption bands are still present in the spectrum (Figure 5e). However the ratio of relative intensities is reversed, showing that the sugars are now mainly in N-type geometry (strong band at 865 cm^{-1}, weak band at 840 cm^{-1}). The presence of one-third of ribose sugars in the structure is not sufficient to explain this inversion. This is clearly shown by the comparison of Figure 5e,f. The amount of S-type sugars (absorption band at 840 cm^{-1}) decreases while that of N-type sugars (absorption band at 865 cm^{-1}) increases when the triple helix is formed. Some of the deoxy sugars in the original duplex adopt now an N-type conformation in the triplex. Figure 3 allows us to assign the N-type geometry in the $^{2'Ome}r(UC^+U_5C^+_6)$*$d(AGA_5G_6)$−$d(C_6T_5CT)$ triple helix besides the riboses to sugars of the polypurine strand. The spectral domain presented contains IR absorption bands characteristic of purine nucleoside geometries, sensitive to sugar pucker modifications. Thus guanosines with sugars

in S-type conformation absorb at 1420 cm^{-1} [for example, B-form poly d(G-C); Taboury et al., 1985] and adenosines at 1425 cm^{-1} [B-form poly d(A-T); Adam et al., 1986]. When sugars adopt an N-type geometry, these absorption bands are shifted to lower wavenumbers. The spectrum of the equimolecular mixture $^{2'Ome}r(UC^+U_5C^+_6)$ + $d(AGA_5G_6)$-$d(C_6T_5CT)$ at pH 7 (Figure 3, solid line) shows a strong absorption band at 1419 cm^{-1}, characteristic of purines with S-type sugars (the absorption band at 1407 cm^{-1} is assigned to a third-strand uracyl vibration). When the triple helix is formed (Figure 3, dashed line), the 1419 cm^{-1} absorption band is no longer detected and the relative intensity of the 1407 cm^{-1} absorption band increased due to the overlap of the uracyl vibration and the vibration of purines with N-type sugars. Purine strand sugars have been forced into a N-type conformation by fixation of the third ribose strand.

DISCUSSION

We have shown by FTIR spectroscopy that it is possible to form triple helices by addition to the $d(AGA_5G_6)$-$d(C_6T_5CT)$ duplex containing the polypurine tract of Friend murine retrovirus of any of the following third strands: $d(TCT_5C_6)$, $d(T^{5me}CT_5{}^{5me}C_6)$, or $^{2'Ome}r(UCU_5C_6)$. We observe that the triple helices prepared with a third strand containing deoxy sugars are obtained at higher pH than when the $^{2'Ome}r(UCU_5C_6)$ oligomer is used as third strand, which can be correlated with the higher p*K* value of deoxycytidine when compared to cytidine. However, once formed, the stabilities of the triplexes are in the opposite order: by increasing the pH, both deoxy*deoxy−deoxy triple helices are denatured before the ribo*deoxy−deoxy triple helix.

Infrared spectroscopy allows us to precisely determine the geometry of the formed triple helices. The presence of a cytosine contribution above 1700 cm^{-1} in the spectra of all triplexes studied here reflects a Hoogsteen-type base-pairing scheme of the third strand oriented parallel with respect to the polypurine tract (Ouali et al., 1993). Moreover the sugar conformations found in these triplexes depend on the nature of the third strand. This is in agreement with our earlier studies concerning intermolecular triplexes formed by addition of a rU_n strand to a dA_n-dT_n duplex or of an rC^+_n strand to a dG_n-dC_n duplex (Liquier et al., 1991; Akhebat et al., 1992). In the first triplex, $(rU*dA-dT)_n$, both N- and S-type sugars were found, while in the second one, $(rC^+*dG-dC)_n$, only N-type sugars were observed. Thus it seems reasonable, when both types of triplets rU*dA−dT and rC^+*dG−dC are present in the sample, to find an important contribution of N-type sugars. A similar result has been recently obtained in our laboratory concerning intramolecular triplexes obtained by folding in acidic pH conditions of a chimeric DNA−RNA 29mer d(GAGAGAA)d(CCCC)-d(TTCTCTC)d(TTTT)−r(CUCUCUU). This oligomer forms a triple helix with two loops, d(CCCC) and d(TTTT). In this case the sugars also mainly adopt an N-type conformation though in the corresponding duplex d(GAGAGAA)-d(CCCC)d(TTCTCTC) they were initially in an S-type geometry (Liquier et al., 1995).

Thermal dissociation followed by UV absorbance spectroscopy has also shown different behavior depending on the third strand used. This is in agreement with recent studies performed by UV absorbance spectrophotometry, gel retardation assays, and molecular modeling concerning the relative stabilities of triple helices that contain strands with either ribose or deoxyribose sugars (Roberts & Crothers, 1992; Escudé et al., 1993; Han & Dervan, 1993; Wang & Kool, 1995). The intermolecular triplex formed by three separate strands (R*D−D) presents a monophasic transition as when a single ribose (R) strand is bound to a DNA hairpin duplex (D−D) (Roberts & Crothers, 1992) and as in the case of the intramolecular triplex formed by folding of the chimeric RNA−DNA molecule presented above. If we consider now triple helices prepared with a deoxy third strand (D) [either $d(TCT_5C_6)$ or $d(T^{5me}CT_5{}^{5me}C_6)$], biphasic melting is observed as previously reported for interstrand (D*D−D) triplexes (Pilch et al., 1990; Miller & Cushman, 1993; Fossella et al., 1993). Comparison of half-dissociation temperatures shows the influence of the nature of the third-strand sugar moieties on triple-helix stability. The formed complexes were found to have stabilities decreasing in the order R*D−D, ^{5me}D*D−D, D*D−D. Substitution of a DNA third strand by an RNA results in a shift of the temperature of third-strand dissociation by 28 °C. The loss of the methyl group from T and the addition of the 2′-hydroxyl group are supposed to favor formation of hydrogen bonds between the third-strand 2′-OH group and the purine strand phosphates, hence a stabilization of R*D−D structure when compared to D*D−D. In our case, such a mechanism cannot be considered as methyl substitution on the 2′-OH groups in the third strand prevents such hydrogen-bonding interactions. The nevertheless observed important stabilization may be due to van der Waals interactions involving the methyl groups, compensating for the loss of hydrogen bonding interactions.

Comparison of the denaturation of triplexes prepared with a deoxy third strand shows that C_5 methylation of the cytosines induces a shift of 7 °C in the T_m. A proposed explanation for this behavior is that these methyl groups form a spine of hydrophobic interactions, which contributes to triple-helical stability (Sun & Hélène, 1993).

In summary, our work shows that it is possible to form pH dependent triple helices targeting the polypurine tract of the Friend murine retrovirus using either deoxy- or ribo-oligonucleotides. 2′-*O*-Methylation of the ribose which may minimize RNAse degradation in possible in vivo applications does not interfere with triple-helix formation. Sugar conformations in the triplexes considered are directly related to the type of sugar (ribose or deoxyribose) present in the third strand. Thus a third strand containing riboses imposes an N-type geometry for the purine strand sugars, even if the initial duplex structure presented S-type sugars.

REFERENCES

Adam, S., Liquier, J., Taboury, J., & Taillandier, E. (1986) *Biochemistry 25*, 3220−3225.

Akhebat, A., Dagneaux, C., Liquier, J., & Taillandier, E. (1992) *J. Biomol. Struct. Dyn. 10*, 577−588.

Dagneaux, C., Liquier, J., Scaria, P. V., Shafer, R. H., & Taillandier, E. (1994) in *Structural Biology: The State of the Art*, Proceedings of the 8th Conversation in the Discipline Biomolecular Dynamics, Albany, NY, June 22−26, 1993 (Sarma, R. H., & Sarma, M. H., Eds.) pp 103−113, Adenine Press, Guilderland, NY.

de los Santos, C., Rosen, M., & Patel, D. (1989) *Biochemistry 28*, 7282−7289.

Escudé, C., Sun, J. S., Rougée, M., Garestier, T., & Hélène, C. (1992) *C. R. Acad. Sci., Sér. 3, 315*, 521−525.

Escudé, C., François, J.-C., Sun, J. S., Ott, G., Sprinz, M., Garestier, T., & Hélène, C. (1993) *Nucleic Acids Res. 21*, 5547−5553.

Fasman, G. D. (1975) in *Handbook of Biochemistry and Molecular Biology*, Vol. 1, p 597, CRC Press, Cleveland, OH.
Fossella, J. A., Kim, Y. J., Shih, H., Richards, E. G., & Fresco, J. R. (1993) *Nucleic Acids Res. 21*, 4511−4515.
Friend, C. (1957) *J. Exp. Med. 105*, 307−318.
Han, H., & Dervan, P. B. (1993) *Proc. Natl. Acad. Sci. U.S.A. 90*, 3806−3810.
Han, H., & Dervan, P. B. (1994) *Nucleic Acids Res. 22*, 2837−2844.
Howard, F. B., Miles, H. T., Liu, K., Frazier, J., Raghunathan, G., & Sasisekharan, V. (1992) *Biochemistry 31*, 10671−10677.
Klinck, R., Guittet, E., Liquier, J., Taillandier, E., Gouyette, C., & Huynh-Dinh, T. (1994) *FEBS Lett. 355*, 297−300.
Liquier, J., Coffinier, P., Firon, M., & Taillandier, E. (1991) *J. Biomol. Struct. Dyn. 9*, 437−445.
Liquier, J., Dagneaux, C., & Taillandier, E. in (1993) Proceedings of the 5th International Conference on the Spectroscopy of Biological Molecules (Theophanides, T., Anastassopoulou, J., & Fotopoulos, N., Eds.) pp 51−54, Kluwer Academic Publishers, Dordrecht, The Netherlands.
Liquier, J., Taillandier, E., Klinck, R., Guittet, E., Gouyette, C., & Huynh-Dinh, T. (1995) *Nucleic Acids Res. 23*, 1722−1728.
Mc Donald, C. D., & Maher, L. J., III. (1995) *Nucleic Acids Res. 23*, 500−506.
Miller, P. S., & Cushman, C. D. (1993) *Biochemistry 32* 2999−3004.
Ouali, M., Letellier, R., Adnet, F., Liquier, J., Sun, J. S., Lavery, R., & Taillandier, E. (1993) *Biochemistry 32*, 2098−2103.
Pilch, D. S., Brousseau, R., & Shafer, R. H. (1990) *Nucleic Acids Res. 18*, 5743−5750.
Povsic, T. J., & Dervan, P. B. (1989) *J. Am. Chem. Soc. 111*, 3059−3061.
Radhakrishnan, I., & Patel, D. J. (1994a) *Biochemistry 33*, 11405−11416.
Radhakrishnan, I., & Patel, D. J. (1994b) *J. Mol. Biol. 241*, 600−619.
Rajagopal, P., & Feigon, J. (1989) *Nature 339*, 637−640.
Roberts, R. W., & Crothers, D. M. (1992) *Science 258*, 1463−1466.
Semerad, C. L., & Maher, L. J., III. (1994) *Nucleic Acids Res. 2*, 5321−5325.
Shimizu, M., Konishi, A., Shimada, Y., Inoue, H., & Ohtsuka, E. (1992) *FEBS Lett. 302*, 155−158.
Sun, J. S., & Hélène, C. (1993) *Curr. Opin. Struct. Biol. 3*, 345−356.
Taboury, J., Liquier, J., & Taillandier, E. (1985) *Can. J. Chem. 63*, 1904−1909.
Taillandier, E., & Liquier, J. (1992) Infrared Spectroscopy of DNA in *Methods in Enzymology* (Lilley, H. J., & Dahlberg, J. J., Eds.) Vol. 211, pp 307−335, Academic Press, New York.
Wang, S., & Kool, E. T. (1994) *Nucleic Acids Res. 22*, 2326−2333.
Wang, S., & Kool, E. T. (1995) *Nucleic Acids Res. 23*, 1157−1164.

BI951515J